Respiratory motion artefact in the liver dome on FDG PET/CT: comparison of attenuation correction with CT and a caesium external source

Dimitri Papathanassiou, Stéphanie Becker, Roland Amir, Benoît Menéroux, Jean-Claude Liehn

Service de Médecine Nucléaire, Institut Jean Godinot, 1 avenue du Général Kœnig, B.P. 171, 51056 REIMS Cedex, France

Received: 3 February 2005 / Accepted: 22 May 2005 / Published online: 31 August 2005

Abstract. *Purpose:* Respiratory motion has been reported to be a potential cause of artefacts on PET/CT, and of errors in the quantification of lesion activity due to inaccurate attenuation correction. We examined FDG images corrected for attenuation with CT and a caesium external source in the same patients to study this artefact and to assess its impact on detection of lesions in the upper part of the liver.
Methods: A total of 122 patients underwent the examination using both attenuation correction techniques, with the Gemini PET/CT scanner. No breathing instructions were given. The images obtained were visually compared, and standardised uptake values (SUVs) in 35 lesions were measured (mean SUV/normal liver SUV) in 14 patients with lesions in the upper part of the liver (less than 5 cm from the upper border).
Results: CT-corrected images of the liver included an artefactual cold area in 84 patients (69%); this area was located in the posterior upper part of the liver (65 patients, 53%), included the top of the liver (ten patients, 8%) or affected both the top and the posterior part (nine patients, 8%). In lesions (and also in normal liver outside the artefactual area), SUVs obtained with CT correction were higher than those obtained with Cs correction ($p<0.05$), though this was usually without relevance for lesion detection. However, in patients with lesions situated inside the artefactual area, SUVs were lower with CT correction, and ability to detect two lesions (6%) was affected.
Conclusion: Failure to detect a liver lesion (especially in the superior and posterior parts) is a rare but possible pitfall when using only CT-corrected FDG images.

Dimitri Papathanassiou (✉)
Service de Médecine Nucléaire,
Institut Jean Godinot,
1 avenue du Général Kœnig,
B.P. 171, 51056 REIMS Cedex, France
e-mail: d.papathanassiou@reims.fnclcc.fr
Tel.: +33-032-6504316, Fax: +33-032-6504339

Keywords: PET/CT – FDG – Attenuation correction – Respiratory motion artefact – Liver lesion

Eur J Nucl Med Mol Imaging (2005) 32:1422–1428
DOI 10.1007/s00259-005-1868-y

Introduction

The introduction of positron emission tomography/computed tomography (PET/CT) in clinical routine has led to the acquisition of more accurate information in investigations using FDG, especially in terms of lesion localisation; this has unquestionable clinical advantages, but the technology ineluctably suffers from artefacts of its own [1]. One of the most prominent artefacts encountered when using PET/CT is due to respiratory motion, which may cause the diaphragm to occupy a different position on the image obtained with CT and the image obtained with PET. In fact, the latter is acquired during many respiratory cycles, leading to an averaged position of the diaphragm on the final PET image, whereas the faster spiral CT acquisition captures the diaphragm in a single position which may be different from the mean position, or in the course of respiratory motion. This phenomenon not only sometimes provokes misregistration of lesions between the two modalities [2–6] or disrupts image fusion of normal organs [7], but also may cause erroneous attenuation correction [8–10]. The density of a particular organ (for example, the low attenuation coefficient of the lung) is then attributed to an area whose real density is different (such as the liver, which has a higher attenuation coefficient than lung). If the diaphragm is lower on the CT image, this results in insufficient correction of the attenuation for the liver dome, leading to a cold area in this zone. This phenomenon has been observed and quantified in as many as 84% of PET/CT studies [11], but is considered not to be diagnostically relevant in most patients. However, a case has recently

been reported [12] in which a liver metastasis not seen with CT attenuation correction was obvious when attenuation correction was performed by means of a transmission scan using an external source. In order to evaluate the impact of motion artefacts in this context, we acquired both CT and transmission (with a caesium external source) scans to correct for attenuation in a series of patients. This approach allowed: (a) characterisation of the frequency and pattern of artefacts in the liver, based on comparison of images assumed to be free of artefact (corrected for attenuation using the external source transmission map) and images possibly subject to artefact (corrected using CT images), and (b) observation of differences in lesion appearance according to the correction method used. In patients with lesions in the upper part of the liver, we evaluated the ability to detect abnormal uptake on the two image sets by visual examination and by comparison of the measured standardised uptake values (SUVs) obtained with the two correction methods. These investigations revealed potential mistakes with PET/CT that we believe need to be kept in mind in order to avoid relatively rare but possible false negative results of PET/CT.

Materials and methods

Patients

Out of a population of 700 patients who were examined with ^{18}F-fluorodeoxyglucose (FDG) PET/CT scan for known or suspected malignancy, 122 patients underwent a short transmission acquisition centred on the liver and diaphragm. These 122 patients were not selected on the basis of any particular criteria except for the possibility that lesion detection may have been affected by the artefact, and they are representative of the population referred for PET/CT in our institution.

The patients (84 males, 38 females) were aged between 17 and 84 years (mean 56). Malignancies were colorectal (30), lung (24), breast (9), head and neck (5), renal (4), ovarian (2), pancreatic (2), hepatocellular (2), pleural (2), thyroid (1) and adrenocortical (1) carcinomas, 18 lymphomas, 2 melanomas, 1 angiosarcoma and 3 cancers with an unknown primary; 16 patients were referred for evaluation of a suspicious lung lesion.

The transmission scan was performed because a lesion was known or suspected in the liver (38 cases, 31%), at the lung base (23, 19%) or in another organ (mainly the spleen) (13, 11%), or because the inspection of non-attenuation-corrected images (which were the first to be reconstructed in our acquisition protocol) led to suspicion of an abnormality in the vicinity of the diaphragm in 48 cases (39%). Although the effect of respiratory motion on lung base or spleen lesions is noteworthy, we focussed our report on the liver because respiration-induced attenuation artefacts on PET/CT in patients with lung lesions have already been studied by others [8], and focal spleen lesions were less frequent than liver metastases in this population.

Quantitative assessment of the SUV in lesions was undertaken for 14 subjects whose FDG PET images revealed lesions in the upper part of the liver. Primary cancers in these subjects were nine colorectal, one lung, one breast, one kidney, one ovarian and one melanoma. Only lesions situated less than 5 cm from the upper liver limit were included in this part of the study.

PET/CT

All patients fasted at least 6 h before FDG injection. They rested lying quietly for 30–45 min before and 60–75 min after they received an intravenous injection of 5 MBq/kg of ^{18}F-FDG.

Studies were performed with the Gemini PET/CT scanner (Philips). CT parameters were: two detector rows, slice thickness 6.5 mm, increment 5 mm, pitch 1.5, rotation time 0.5 s, table speed 30 mm/s. For spiral acquisition from the base of the skull to the thigh, the total duration of CT scanning was about 30 s. Using 100 mAs and 120 kV, the computed tomography dose index (CTDI) was 7.3 mGy. The 3D PET emission acquisition parameters were: eight to ten steps covering the body from the thigh to the skull, with a duration of 3 min for each step. PET transmission scans were obtained with a ^{137}Cs source, for two or three steps of 21 s each. This additional procedure lengthened the total examination time typically by less than 3 min. No instructions for breathing were given to the patients.

The non-corrected images were reconstructed first, with a 2D-RAMLA algorithm. Image reconstruction used the 3D-RAMLA algorithm for both the attenuation-corrected volumes. Attenuation-corrected images were displayed using a normalised scale in which grey levels corresponded to the SUV.

In the following, the images corrected for attenuation using the external ^{137}Cs source and using the CT acquisition are referred to as Cs-corrected and CT-corrected respectively.

Image analysis

Assessment of the artefact for each patient was made by the same observer, who also detected the lesions and drew regions of interest (ROIs).

Evaluation of artefact patterns CT-corrected and Cs-corrected images were analysed side-by-side in axial, coronal and sagittal planes, throughout the liver volume. Differences evident visually were considered significant, and artefacts were classified depending on the shape of the cold area on the CT-corrected image that was absent on the Cs-corrected image.

Detection of liver dome lesions During the side-by-side analysis of the two sets of corrected images, areas of increased focal uptake were sought. Whatever correction technique was used, visually significant abnormal uptake was considered a positive result. Images of the patients selected for quantitative assessment of the SUV were reviewed by another observer, blind to the clinical context. When it was uncertain whether a lesion was present in the upper part of the liver, a consensual interpretation was obtained between the two observers.

Quantitative assessment of liver dome lesions SUVs were obtained with the manufacturer's software, using a circular ROI encompassing the lesion. Values studied were the mean SUV in the ROI (SUV per body weight). The ROI size was then adapted to each lesion, but was the same for CT- and Cs-corrected images. The measurement was done in the slice where the maximum intensity was encountered for each lesion in the two modalities. This slice was usually the same for CT- and Cs-corrected images. We also used a ROI to represent normal liver, drawn in a region free of lesion and unlikely to be involved in the artefact; this ROI was often located in another slice than the lesion. The same ROI position was chosen for both modalities; the size of this ROI was the same for all the patients.

Statistical analysis

Two-tailed paired *t* test was used for comparison of values obtained with the two attenuation correction techniques. Other comparisons were performed using unpaired *t* test or *Z*-score calculation.

Results

Patterns of artefact

A different appearance of the liver when using the two attenuation correction methods was observed in 84 patients (69%). Four main patterns of artefact were found on the CT-corrected images compared with the Cs-corrected images. The first pattern was a curvilinear cold area including the top of the liver, of variable severity, which we refer to as type 1. Nine patients presenting type 1 artefacts had an obvious association with some of the following patterns. Types 2–4 were cold areas most frequently situated in the posterior and internal parts of the upper liver (segments IV, VII, VIII). In place of the dome, a slope from the top to the posterior part was visible on the sagittal slices, or a concave curve (or less convex curve than the normal dome) was present, or a cold area seemed to enter the liver. Figure 1 shows representative examples of the four types. In type 1 the whole superior edge of the liver seems to shift downwards on the coronal and sagittal slices. In type 2 the posterior part of the liver, but not necessarily the top, is affected by the artefact. In type 3 a large portion of the posterior and often the internal part of the liver appears cold; the aspect of a "stair" is to be noted on the sagittal (and often the coronal) slice. In type 4 the cold area enters under the top of the liver on the sagittal slice and gives rise to a "mushroom" shape on the coronal slice. Table 1 gives the frequencies of each artefact.

Lesion detection

In 14 patients, 35 hepatic lesions were found in the upper part of the liver. In most cases, the visual characteristics of the lesion relevant to detectability were similar whichever correction method was used. However, for lesions located in the cold area due to artefact (only three lesions were in the cold area), intensity appeared lower on CT-corrected than on Cs-corrected images. Two such lesions might have been considered non-significant on CT-corrected images, but appeared significant on Cs-corrected images. One of these lesions is shown in Fig. 2: it was not easily detected on the CT-corrected images. Inspection of the non-corrected images led to the expectation that an area of abnormal uptake would be visible on the corrected images. However, this did not always prove to be the case, and if an abnormal focus was visible, the observer could falsely localise it to the lung base.

Standardised uptake values

SUVs measured in the lesions were found to differ between CT-corrected and Cs-corrected images (mean±SD: 4±1.31 and 3.75±1.07, respectively) when the 35 lesions in 14 patients were pooled ($p<0.05$). However, SUVs in the normal liver in these patients also differed depending on the correction modality (mean±SD: 2.53±0.45 and 2.07±0.44 for CT-corrected and Cs-corrected images, respectively; $p<10^{-9}$).

Because SUVs were higher with CT correction than with Cs correction, we investigated the ratio of lesion SUV to normal liver SUV as a measure of the contrast, relevant to lesion detectability. This ratio was higher with Cs-corrected images ($p<0.01$). Of the three lesions situated in the cold area due to artefact, two exhibited significantly lower values compared with other lesions on CT-corrected images ($|Z| > 1.96$), but not on Cs-corrected images. For these three lesions, ratio values (mean±SD, range) were 0.81±0.52 (0.31–1.35) and 1.51±0.29 (1.28–1.83) with CT correction and Cs correction, respectively, while they were 1.76±0.62 (0.92–3.53) and 1.97±0.65 (1.05–3.81) for the 32 other lesions.

Discussion

We took advantage of the possibilities offered by the Gemini device to correct the emission images of the same patients using attenuation maps either derived from the CT acquisition or obtained with the external ^{137}Cs source, and then to compare images with a possible respiratory motion artefact and those without an artefact a priori. The transmission acquisition proved a powerful tool to study the impact of respiratory motion during CT acquisition. We found it to be easy to perform and not time consuming. The additional equivalent dose is low compared with the total equivalent dose due to the PET/CT procedure.

Assessment of the impact of the artefact in patients with liver lesions was hindered by the rather small size of the population: the artefact was observed to have a dramatic effect in only two patients (three lesions out of 35). This might have been because it is a relatively rare occurrence for a lesion to be located exactly in that part of the liver subject to artefact. The two patients represented a small minority of the 14 patients with lesions in the upper part of the liver (less than 5 cm from the upper border), who themselves numbered less than one-half of those with a lesion anywhere in the liver. It is to be noted that in the aforementioned two patients the existence of the lesions was confirmed by a modality other than PET (MRI or CT scan).

We used no breathing protocol in this study. In addition to respiratory gating techniques or software methods that aim to minimise differences between CT and PET liver images, such protocols (which are all the more feasible owing to the speed of CT acquisition) appear a useful means to reduce the effects of motion artefact.

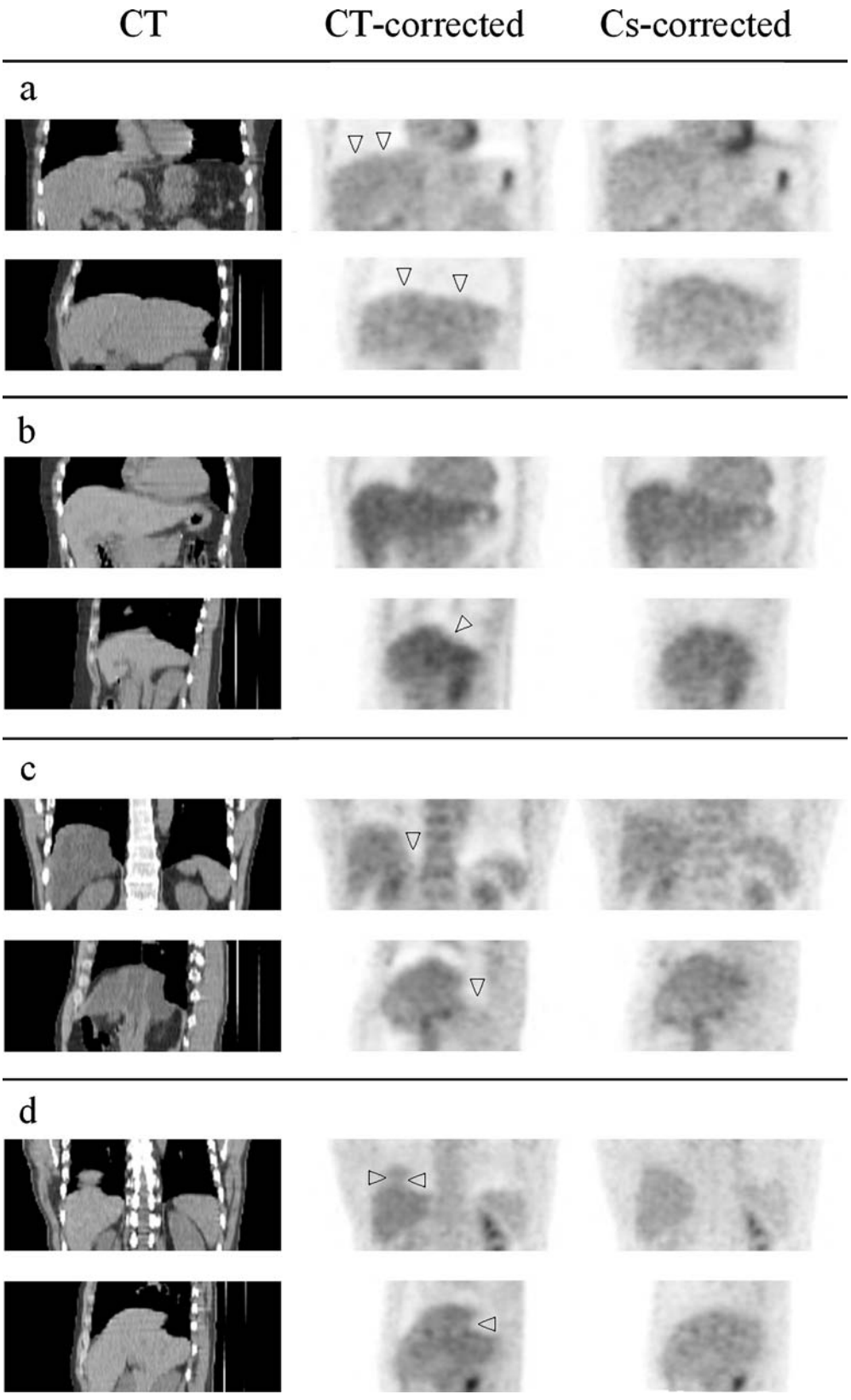

Fig. 1. Examples of the main patterns of artefact. **a** type 1; **b** type 2; **c** type 3; **d** type 4. For each type, representative coronal and sagittal slices (*top and bottom rows*, respectively) are shown for the same level in CT images and CT-corrected and Cs-corrected PET images (*left, middle and right columns*, respectively). Artefact on CT-corrected images is indicated by *open arrowheads*. (On **a**, an associated type 4 artefact is also visible on the sagittal CT image.)

Frequency and patterns of artefact

It has already been reported [11] that motion artefact is very frequent when no breathing protocol is applied. Our study confirms that the phenomenon occurs in more than two-thirds of patients.

Interestingly, we observed that the artefacts most often described elsewhere were not those most frequently en-

Table 1. Number of patients whose images were affected by the different types of artefact

Type	Number	Percentage of the total population	Percentage of the population with artefacts
1 only	10	8	12
1+2	2	2	2
1+3	6	5	7
1+4	1	1	1
2 only	11	9	13
3 only	44	36	52
4 only	10	8	12
Total type 1	19	16	23
Total type 2	13	11	15
Total type 3	50	41	60
Total type 4	11	9	13

countered in our study. The literature on artefacts due to respiratory motion contains frequent references to a curvilinear cold area (which we called type 1) [11, 13] or "mushroom" artefacts (which we called type 4) [14, 15]. However, in our experience, artefacts affecting the posterior part or the posterior and internal parts of the liver, resulting in apparent absence of a part of the organ with a variable obtuse angle shape on sagittal images (types 2 and 3), occur in close to one-half of patients. The frequency of type 2 and 3 artefacts leads us to think that the posterior part of the dome is particularly subject to motion artefact, which contrasts with the finding in another study [11] that the distance between the top and bottom of the artefact was less in the posterior part of the liver (13.6 mm) than in the middle (14.3 mm) or anterior (16.4 mm) parts; these were mean values in 50 patients, however.

It needs to be pointed out that the classification employed in the present study does not directly take into account the severity of the artefact (in terms of the liver volume involved in the cold area), but rather is essentially based on its shape.

Type 1 artefacts might be due to two phenomena: (1) a constant position of the diaphragm during CT acquisition that is different from the mean position during PET acquisition, or (2) movement of the diaphragm during CT acquisition, but without any visible effect on the imaging of the liver border. The latter was most likely in our study, though because we gave no instructions to the patients it is impossible to assert whether the position of the diaphragm was constant or not. Nevertheless the effect of the artefact would likely be the same if the diaphragm position was constant. Artefacts of types 2, 3 and 4 are obviously due to the movement of the diaphragm during the acquisition of CT slices: a part of the dome is caught on the upper slices, and then the dome moves down and subsequent slices do not capture some of the liver (often the posterior and internal parts). Breathing protocols [10,

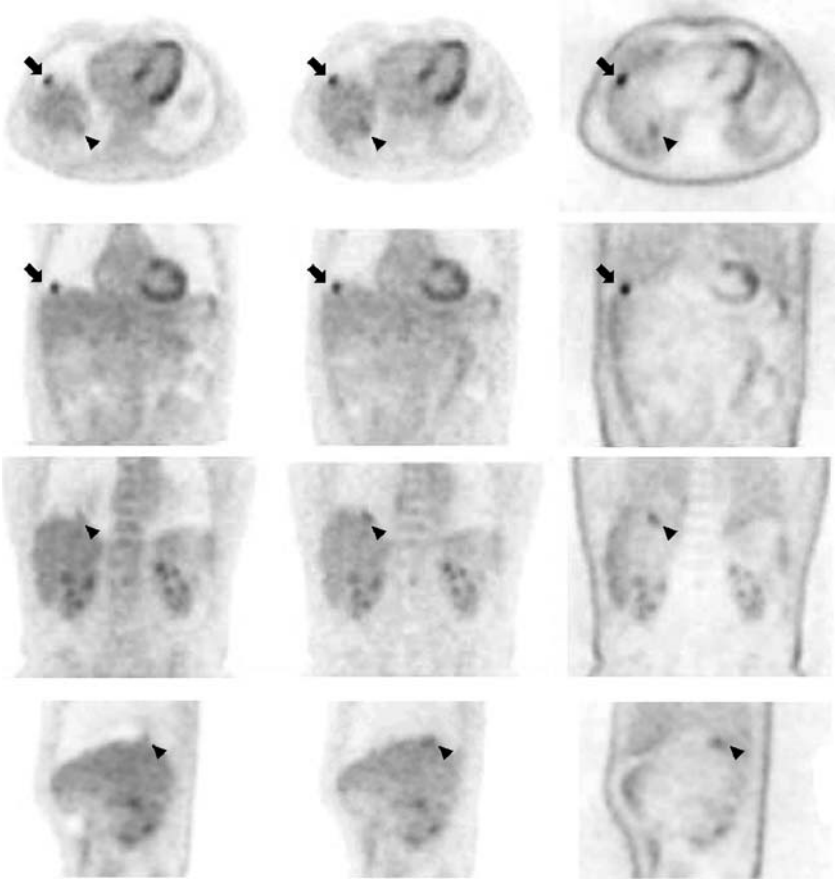

Fig. 2. In this patient, two lesions were located in the artefact area: an anterior lesion (*arrow*) and a posterior lesion (*arrowhead*) are present in the upper part of the liver. Shown are axial slices (*top row*), coronal slices at two different levels (*second and third rows*) and sagittal slices (*bottom row*) of CT-corrected images (*left column*), Cs-corrected images (*middle column*) and non-corrected emission images (*right column*)

14, 16–18] have proved useful in reducing motion artefacts. The relevance of the optimisation of the CT part of a hybrid PET/CT investigation then arises. However, while such protocols might avoid artefacts of types 2–4, which appear as variants of the same phenomenon, they might not avoid type 1 artefacts if breath hold does not correspond to the mean diaphragm position. Moreover, type 1 artefacts seem more challenging than artefacts of types 2–4 because if the cold area is spatially narrow and visually not severe, there are fewer clues that an artefact is affecting attenuation correction.

Lesion detection

The sole purpose of this study was to compare the two attenuation correction methods. As a consequence, the process of lesion detection may seem somewhat artificial, in that non-corrected images were not taken into account. Careful inspection of non-corrected images remains mandatory to avoid misinterpretations due to artefacts [1], and its relevance is highlighted by our results. However, non-corrected images may sometimes be misleading if they show an abnormality that appears to be located in the lung. CT images may then help because in such cases no lung lesion is visible; the combination of information elements may thus resolve some problems, though this is not so in every case (liver lesions are not necessarily revealed on non-contrast-enhanced CT images acquired during a PET/CT session). One may sometimes remain unable to localise a small lesion in the vicinity of the liver border with non-corrected and CT-corrected images. Furthermore, according to our results, lesion SUV may be impaired on CT-corrected images. Use of both attenuation correction methods in the same patients is not relevant in most cases, but it may be of help in doubtful cases (when low uptake is visible on non-corrected images) or if SUV follow-up is required.

Standardised uptake values

Differences in SUVs between images corrected for attenuation using CT and those corrected for attenuation using an external source have previously been observed with ^{68}Ge [19, 20]; they are probably attributable in part to differences in the attenuation process and in attenuation coefficient evaluation [21] caused by differences in the photon energies. We found different values between modalities for lesions and for normal liver. Interestingly, though the SUVs were highest with CT-corrected images, the ratio of lesion SUV to normal liver SUV was better with Cs-corrected images. We used this ratio in an attempt to quantify contrast between lesion and normal tissue. However, this does not mean that the contrast is always less marked on CT-corrected images: actually, in some cases satisfactory visual contrast may be observed on CT-corrected images, thanks partly to the presence of more readily apparent lung tissue (relatively cold) around the hot spot corresponding to the lesion.

Artificial lowering of the SUV due to lesion movement is caused by inadequate attenuation correction or by a blurring effect during acquisition. The latter factor could not be addressed in our study, because whatever attenuation correction method was used, the emission acquisition was the same. Differences in SUV depended on the presence or absence of tissue (tumour or liver), not on discrepancies in lesion position between emission and transmission or CT images, which could be the source of SUV differences in the case of pulmonary lesions (we assume that the densities of tumour and normal liver parenchyma are more similar than those of tumour and normal lung). Alterations in SUV measurement due to respiratory motion have been observed in other studies [9, 10, 22] when the source of PET signal and tissue in CT images are misregistered. One of the main results of our study is that the SUVs of liver lesions situated in the artefact area were clearly lowered because of the artefact. When the lesion was not inside the artefact area, no substantial effect was noted, even if the lesion was close to the diaphragm.

Conclusion

The comparison of images corrected for attenuation using either CT or a caesium external source enabled us to describe different patterns of motion respiratory artefact and to assess its frequency. We also observed an effect on SUV when lesions were located in the artefact area; this seems not to be a frequent occurrence, but it is encountered in clinical practice. Beyond being an interesting technical approach for the study of such artefacts, the short transmission acquisition may be of value in some cases in clinical practice until respiratory gating [23] achieves daily use, and it may offer complementary information when doubt exists regarding the region surrounding the diaphragm. Nuclear medicine physicians interpreting PET/CT images must be aware of the possibility not only of misinterpretation of lesion location, but also of a reduction in lesion intensity due to the artefact. As emphasised in this study, avoidance of such a potential source of error reduces the possibility of a false negative PET/CT result.

Acknowledgements. The authors thank S. Baudet, C. Cossus, C. Marques, F. Nicolats and I. Patouillard for their valuable help in the acquisition and processing of the data used in the present study, and L. Gausachs for provision of information on the Gemini device.

References

1. Bockisch A, Beyer T, Antoch G, Freudenberg LS, Kuhl H, Debatin JE et al. Positron emission tomography/computed tomography—imaging protocols, artifacts, and pitfalls. Mol Imaging Biol 2004;6:188–99

2. Osman MM, Cohade C, Nakamoto Y, Marshall LT, Leal JP, Wahl RL. Clinically significant inaccurate localization of lesions with PET/CT: frequency in 300 patients. J Nucl Med 2003;44:240–3
3. Goerres GW, Kamel E, Seifert B, Burger C, Buck A, Hany TF et al. Accuracy of image coregistration of pulmonary lesions in patients with non-small cell lung cancer using an integrated PET/CT system. J Nucl Med 2002;43:1469–75
4. Cohade C, Osman M, Marshall LN, Wahl RN. PET-CT: accuracy of PET and CT spatial registration of lung lesions. Eur J Nucl Med Mol Imaging 2003;30:721–6
5. Sarikaya I, Yeung HW, Erdi Y, Larson SM. Respiratory artefact causing malpositioning of liver dome lesion in right lower lung. Clin Nucl Med 2003;28:943–4
6. Cook GJ, Wegner EA, Fogelman I. Pitfalls and artifacts in ^{18}FDG PET and PET/CT oncologic imaging. Semin Nucl Med 2004;34:122–33
7. Nakamoto Y, Tatsumi M, Cohade C, Osman M, Marshall LT, Wahl RL. Accuracy of image fusion of normal upper abdominal organs visualized with PET/CT. Eur J Nucl Med Mol Imaging 2003;30:597–602
8. Goerres GW, Burger C, Kamel E, Seifert B, Kaim AH, Buck A et al. Respiration-induced attenuation artifact at PET/CT: technical considerations. Radiology 2003;226:906–10
9. Chin BB, Nakamoto Y, Kraitchman DL, Marshall L, Wahl R. PET-CT evaluation of 2-deoxy-2-[^{18}F]fluoro-D-glucose myocardial uptake: effect of respiratory motion. Mol Imaging Biol 2003;5:57–64
10. Visvikis D, Costa DC, Croasdale I, Lonn AH, Bomanji J, Gacinovic S et al. CT-based attenuation correction in the calculation of semi-quantitative indices of [^{18}F]FDG uptake in PET. Eur J Nucl Med Mol Imaging 2003;30:344–53
11. Osman MM, Cohade C, Nakamoto Y, Wahl RL. Respiratory motion artifacts on PET emission images obtained using CT attenuation correction on PET-CT. Eur J Nucl Med Mol Imaging 2003;30:603–6
12. Papathanassiou D, Liehn JC, Bourgeot B, Amir R, Marcus C. Cesium attenuation correction on the liver dome revealing hepatic lesion missed with computed tomography attenuation correction because of the respiratory motion artifact. Clin Nucl Med 2005;30:120–1
13. Cohade C, Wahl RL. Applications of positron emission tomography/computed tomography image fusion in clinical positron emission tomography—clinical use, interpretation methods, diagnostic improvements. Semin Nucl Med 2003; 33:228–37
14. Beyer T, Antoch G, Muller S, Egelhof T, Freudenberg LS, Debatin J et al. Acquisition protocol considerations for combined PET/CT imaging. J Nucl Med 2004;45 Suppl 1:25–35S
15. PET/CT Image Artifacts. In: Czernin J, Dahlbom M, Ratib O, Schiepers C, editors. Atlas of PET/CT imaging in oncology. Berlin Heidelberg New York: Springer; 2004 p. 63–75
16. Goerres GW, Kamel E, Heidelberg TN, Schwitter MR, Burger C, von Schulthess GK. PET-CT image co-registration in the thorax: influence of respiration. Eur J Nucl Med Mol Imaging 2002;29:351–60
17. Beyer T, Antoch G, Blodgett T, Freudenberg LF, Akhurst T, Mueller S. Dual-modality PET/CT imaging: the effect of respiratory motion on combined image quality in clinical oncology. Eur J Nucl Med Mol Imaging 2003;30:588–96
18. De Juan R, Seifert B, Berthold T, von Schulthess GK, Goerres GW. Clinical evaluation of a breathing protocol for PET/CT. Eur Radiol 2004;14:1118–23
19. Nakamoto Y, Osman M, Cohade C, Marshall LT, Links JM, Kohlmyer S et al. PET/CT: comparison of quantitative tracer uptake between germanium and CT transmission attenuation-corrected images. J Nucl Med 2002;43:1137–43
20. Kamel E, Hany TF, Burger C, Treyer V, Lonn AH, von Schulthess GK et al. CT vs. ^{68}Ge attenuation correction in a combined PET/CT system: evaluation of the effect of lowering the CT tube current. Eur J Nucl Med Mol Imaging 2002; 29: 346–50
21. Kinahan PE, Hasegawa BH, Beyer T. X-ray-based attenuation correction for positron emission tomography/computed tomography scanners. Semin Nucl Med 2003;33:166–79
22. Erdi YE, Nehmeh SA, Pan T, Pevsner A, Rosenzweig KE, Mageras G, et al. The CT motion quantitation of lung lesions and its impact on PET-measured SUVs. J Nucl Med 2004; 45:1287–92
23. Nehmeh SA, Erdi YE, Pan T, Pevsner A, Rosenzweig KE, Yorke E et al. Four-dimensional (4D) PET/CT imaging of the thorax. Med Phys 2004;31:3179–86